Gating Protein Transport in Solid State Nanopores by Single Molecule Recognition

N.B. When citing this work, cite the original published paper.

(article starts on next page)

# Gating Protein Transport in Solid State Nanopores by Single Molecule Recognition

Gustav Emilsson,[†] Yusuke Sakiyama,[‡] Bita Malekian,[†] Kunli Xiong,[†] Zeynep Adali-Kaya,[†] Roderick Y. H. Lim,[‡] and Andreas B. Dahlin*,[†]

[†]Department of Chemistry and Chemical Engineering, Chalmers University of Technology, 41296 Göteborg, Sweden
[‡]Biozentrum and the Swiss Nanoscience Institute, University of Basel, 4056 Basel, Switzerland

S Supporting Information

ABSTRACT: Control of molecular translocation through nanoscale apertures is of great interest for DNA sequencing, biomolecular filters, and new platforms for single molecule analysis. However, methods for controlling the permeability of nanopores are very limited. Here, we show how nanopores functionalized with poly(ethylene glycol) brushes, which fully prevent protein translocation, can be reversibly gated to an "open" state by binding of single IgG antibodies that disrupt the macromolecular barrier. On the basis of surface plasmon resonance data we propose a two-state model describing the antibody−polymer interaction kinetics. Reversibly (weakly) bound antibodies decrease the protein exclusion height while irreversibly (strongly) bound antibodies do not. Our results are further supported by fluorescence readout from pore arrays and high-speed atomic force microscopy on single pores. This type of dynamic barrier control on the nanoscale provides new possibilities for biomolecular separation and analysis.
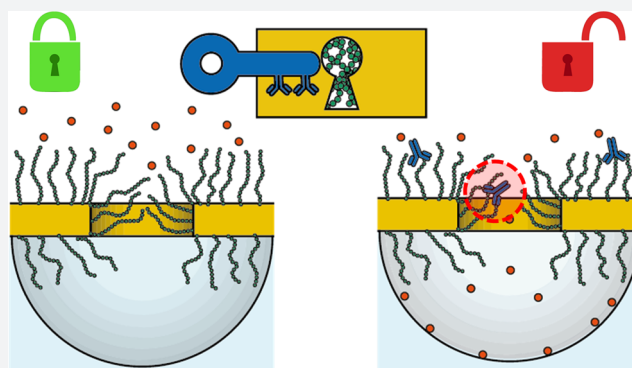
■ INTRODUCTION

Control of molecular translocation through nanochannels or nanopores in thin membranes is central to many aspects of chemical analysis.[1] The most known application is probably detection and potential sequencing of single DNA molecules as they pass through a solid state nanopore, a process which can be analyzed by changes in the ionic conductivity.[2] Another subject of intense research is biomolecular filters based on selective transport through arrays of nanopores, according to molecular size or charge.[3] Such filters have many advantages including high throughput by diffusion alone if the membrane is ultrathin and passive steady-state operation. Further, in contrast to chromatography columns and batchlike separation processes, membranes with defined nanopore arrays may enable parallel separation of multiple analytes and easy implementation in lab-on-a-chip systems. Pioneering studies have shown that chemically modified nanopores may provide separation based on molecular recognition, i.e., a form of facilitated diffusion. For instance, track-etched polycarbonate membranes or anodized alumina combined with proper surface functionalization can provide some degree of specificity with respect to drug enantiomers,[4] proteins,[5] and nucleotide sequences.[6]

However, control of permeability in artificial nanopore systems remains challenging. In all biomolecular filters presented so far, the transport selectivity is low[4−6] (a factor 2−5); i.e., other molecular species are "leaking" through.

Therefore, bottom-up approaches are still far from being able to mimic the remarkable selectivity found in biological nanopores.[7−9] In particular, it remains difficult to *gate* nanopores in a controllable manner, i.e., to switch between an open and a closed state with respect to molecules of interest. The possibility to regulate transport in novel ways can in the long run provide advanced directional and dynamic separation, but existing methods for controlling permeability are based on changing the liquid bulk properties.[10] Even polymer-functionalized nanopore systems utilize changes in bulk solvent quality by pH[11] or temperature,[12] which makes gating slow and excludes local permeability control along a channel. Furthermore, control of transport through nanopores has so far focused on the passage of ionic currents.[13] Regulation of protein translocation by surface chemistry has been limited to nonresponsive and irreversible chemical modifications,[14] which essentially only modify the effective pore diameter.[15]

We have recently established that hydrophilic polymer brushes on the walls of nanopores in ultrathin gold films can form extremely thin "sieve" barriers which efficiently block passage of serum proteins, while still allowing water flow and free diffusion of small molecules (∼1 kDa).[16] In this work we investigate how an IgG poly(ethylene glycol) (PEG) antibody
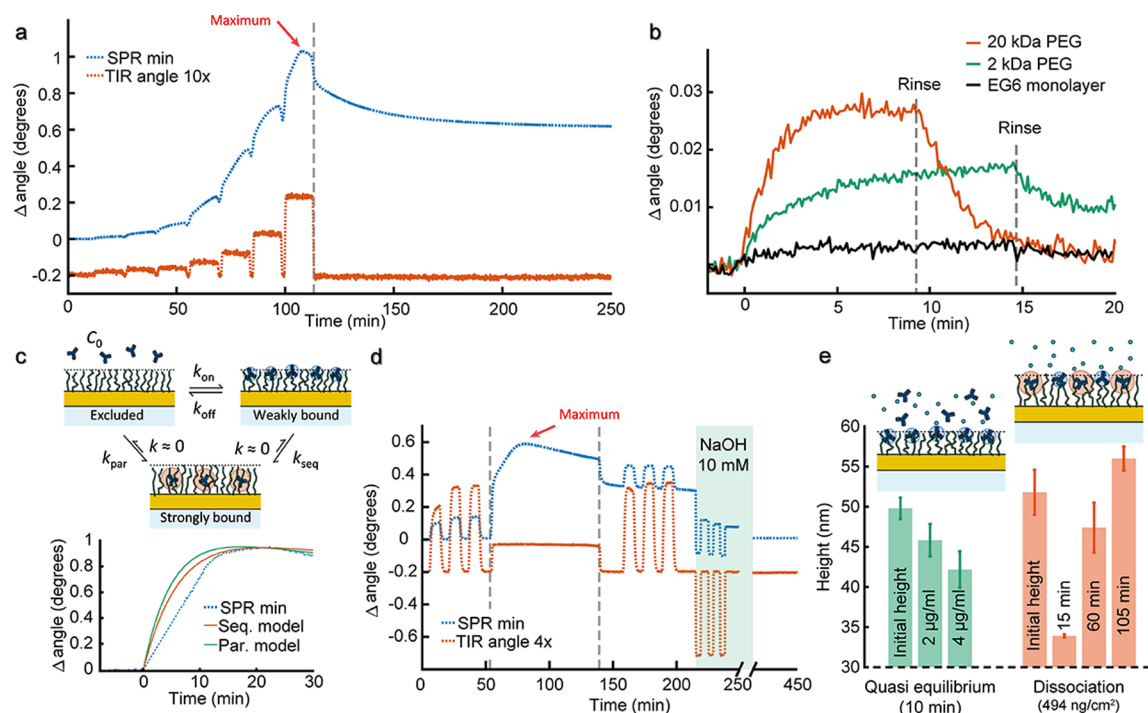
Figure 1. Characterizing the AB−PEG interaction by SPR. (a) Kinetic titration of ABs to a PEG brush. The concentrations injected are 2, 5, 10, 25, 50, 100, and 200 μg/mL. (The TIR angle is shifted and enhanced for clarity.) (b) Association and dissociation kinetics monitored in SPR for 4 μg/mL AB injected on different surfaces. (c) Proposed two-state binding model and example of fitting association phase data. (d) Single injection of 400 μg/mL AB with BSA injections to probe brush height before and after. Eventually the baseline is recovered after washing steps with 10 mM NaOH. (e) Summary of protein exclusion height measurements. The green bars show brush compression due to weakly bound ABs, probed after 10 min. (Injections of BSA were performed while maintaining the same AB concentration.) The red bars show heights at different times during the dissociation phase after first reaching an AB coverage of 494 ng/cm².

(AB) affects this impenetrable barrier as it binds inside the nanoscale apertures. Utilizing the inherent plasmonic activity associated with the nanopores,[17] we show real-time detection of protein translocation and AB interactions with the PEG brush inside the pore. Further, by probing the protein exclusion of the PEG brush with surface plasmon resonance (SPR), dynamic alterations in the brush height caused by the AB are elucidated. Our results are further verified by fluorescence imaging, and high-speed atomic force microscopy (AFM) is used to image morphology changes of the brush inside the pores.

■ RESULTS AND DISCUSSION

Inspired by simulations suggesting the possibility to gate brush-modified nanopores by interactions with additives[18,19] and our previous demonstration of pore sealing by PEG,[16] we hypothesized that ABs which bind to PEG[20−24] would disrupt the barrier and open the pores with respect to proteins. Although the binding of certain antibodies to PEG is established, the details of such interactions and their kinetics appear not to have been studied in detail. Therefore, we first characterized the binding between ABs and PEG brushes on planar gold using SPR. We used the E11 PEG AB which recognizes chains of EG units, i.e., it is "backbone binding".[20] Further, we used thiol-terminated 20 kDa PEG to prepare brushes on gold by grafting in a θ solvent as described previously,[25] reaching a grafting density of 0.28 nm^{-2}.[16]

The titration of ABs to the PEG brush showed a complex behavior for the interaction (Figure 1a). The first anomaly is that at higher concentrations the association phase consistently

showed non-monotonically increasing behavior; i.e., the signal increased quickly initially followed by a slow *decrease*. This was not an artifact due to variations in the bulk refractive index since we also confirmed that the total internal reflection (TIR) angle remained constant.[26] Similar "peaks" in the association phase can be observed in published SPR data for multivalent interactions[27] but apparently remain unexplained. The second peculiarity is that when a considerable amount of AB had become bound (>0.1° signal), the signal no longer returned to the initial value after rinsing (Figure 1a), showing that a fraction of the ABs become irreversibly bound to the brush. Still, at low AB concentrations the signal quickly stabilized and was essentially fully reversible. For instance, Figure 1b shows the association and dissociation of ABs introduced at only 4 μg/mL, also including a comparison for binding to monolayers consisting of 2 kDa PEG or an oligomer with 6 EG units.[25] It is clear that a reasonably long EG chain is needed to detect binding (45 units in 2 kDa). In addition, the thicker PEG brush increases the binding capacity because the signal is higher even though the antibodies should be located further away from the solid surface.[25]

To account for the striking features observed in the binding kinetics we use a two-state binding model which assumes that each AB may interact either "weakly" or "strongly" with the polymer brush, as has been suggested in theoretical predictions.[28] The dynamics can be described either as two *parallel* independent binding processes or by a *sequential* transition from weak to strong binding (Figure 1c). In both cases we assume that there is no dissociation from the strong binding state, in agreement with the partially irreversible SPR

response. The differential equations describing the parallel binding kinetics can be written as

$$\frac{\partial \Gamma_1}{\partial t} = k_{on}C_0[\Gamma_{max} - \Gamma_1(t) - n\Gamma_2(t)] - k_{off}\Gamma_1(t)$$

$$\frac{\partial \Gamma_2}{\partial t} = k_{par}C_0[\Gamma_{max} - \Gamma_1(t) - n\Gamma_2(t)]$$

In this model $k_{seq} = 0$. The equations describing the sequential binding model (where $k_{par} = 0$) are instead written as

$$\frac{\partial \Gamma_1}{\partial t} = k_{on}C_0[\Gamma_{max} - \Gamma_1(t) - n\Gamma_2(t)] - k_{off}\Gamma_1(t)$$
$$- k_{seq}\Gamma_1(t)[\Gamma_{max} - \Gamma_1(t) - n\Gamma_2(t)]$$

$$\frac{\partial \Gamma_2}{\partial t} = k_{seq}\Gamma_1(t)[\Gamma_{max} - \Gamma_1(t) - n\Gamma_2(t)]$$

Here, Γ_1 is the molar surface coverage of weakly bound ABs, Γ_2 the surface coverage of strongly bound ABs, and C_0 the concentration of ABs in solution. Further, Γ_{max} is the hypothetical maximum surface coverage of ABs (number of binding sites) if the strongly bound state would not be available ($k_{par} = k_{seq} = 0$ and $C_0 \rightarrow \infty$). Note that Γ_{max} is unknown, although clearly increasing with the amount of polymer on the surface. (Note also that the rate constants k_{par} and k_{seq} have different dimensions.) Similar models have been proposed for other antibodies to account for avidity at high receptor surface density[29] or to describe heterogeneous binding sites at the surface.[30] Here we introduce the factor n to account for the fact that the strong binding state should "occupy" more of the available PEG. In both models, a strongly bound AB interacts with n times more EG units, or at least makes them unavailable for binding to other ABs.

Each system of two ordinary differential equations above can be solved numerically to obtain the association (or dissociation) kinetics. We first fitted $k_{off} = 1.2 \times 10^{-3}$ s^{-1} using dissociation phase data ($C_0 = 0$) and the parallel model, i.e., a simple exponential decay. Using the sequential model for the dissociation data, thereby allowing a transition to the strongly bound state even when $C_0 = 0$, did not lead to a significantly improved fit. The association phase is more challenging to model as there are several unknown parameters, but a value of $n > 1$ is necessary to reproduce the experimentally observed maxima in the association curves. The physical interpretation is that as the brush becomes crowded, a greater number of weakly bound ABs are being replaced by fewer strongly bound ones. For an IgG AB, it is tempting to use $n = 2$, i.e., a bivalent interaction representing the ScFv regions on the two "arms".[29] However, theory[28] and experiments[22] suggest that the AB interaction with the PEG may be more complex. From Figure 1b it is clear that the AB does not simply recognize a few EG units bound to its tips. Using numerical evaluations we found that, regardless of whether the binding was assumed to be parallel or sequential, the value $n = 3$ gave the best fits to the association kinetics together with a rate constant of $k_{on} = 1.0 \times 10^3$ M^{-1} s^{-1}. Further, $k_{par} = 3.0 \times 10^2$ M^{-1} s^{-1} was fitted for the parallel model and $k_{seq} = 1.2 \times 10^8$ cm^2 s^{-1} for the sequential model. We also fitted Γ_{max} to 5 pmol/cm,^{2} while C_0 always was fixed to its known value (more details in the Supporting Information). On the basis of these results we conclude that as long as C_0 is

on the order of a few μg/mL, and the PEG brush is exposed for less than 1 h, very few antibodies will become strongly bound, and a quasi-equilibrium is established through weak interactions within ~10 min. However, the true equilibrium state according to the models is that the brush only contains strongly bound ABs, although this takes over 24 h to achieve even at high concentrations (Supporting Information). Further, it should be kept in mind that the rate constants are for the 20 kDa PEG brush at $\Gamma = 0.28$ nm^{-2}. Other brushes may exhibit different interaction dynamics with the AB. Indeed, the 2 kDa PEG has some strongly bound ABs even after low exposure (Figure 1b), suggesting that k_{par} and/or k_{seq} is higher in this case.

The SPR system also provides a way to monitor the height of the brush by injecting noninvasive probe molecules, typically bovine serum albumin (BSA), which change the bulk refractive index outside the brush.[16,25,26] The resulting height represents the characteristic distance from the surface below which proteins are excluded from the brush. Using this methodology, we first measured the height of the brush before AB binding and during the dissociation phase (Figure 1d). After exposure to a high concentration ($C_0 = 400$ μg/mL) we initially detected a decrease in height from 50 nm down to 33 nm, even though some dissociation had then already occurred. This is in qualitative agreement with previous studies on other brushes.[24] However, after an additional 20 min of dissociation the height was 47 nm, and at the final probing, when only strongly bound AB remain, the protein exclusion height had *increased* by a few nm, probably due to the volume occupied by the ABs themselves. Measurements of the brush heights after 10 min of exposure to low AB concentrations showed brush compression of up to 10 nm (summary in Figure 1e). During such a short exposure, essentially no ABs become strongly bound, in agreement with the fitted rate constants k_{par} and k_{seq}. In summary the exclusion height data shows that the weakly bound ABs compact the brush while the strongly bound do not. The two types of binding are thus clearly different in nature, and it is confirmed that the strong binding is *not* simply a bivalent version of the weak. Notably, this shows similarities to the interactions associated with transport proteins and disordered peptides in the nuclear pore complex[9] (NPC), but also differences since strong binding is then pronounced at lower surface coverage.[31]

The decrease in brush height due to weakly bound ABs is quite remarkable considering that the number of ABs on the surface is relatively low (cf. response in Figure 1b). From a standard quantification of the SPR response to proteins,[25] the number of IgGs (150 kDa) inside the brush in contact with $C_0 = 4$ μg/mL is at least 200 times less than the number of PEG coils (one per 3.6 nm^2). Since the average exclusion height still decreases by almost 10 nm, each weakly bound AB must have a very strong effect on the *local* brush morphology. Under the assumption that the area of the brush region influenced by one antibody is comparable to its size ($15 \times 9 \times 4$ nm^3), the local height decrease must be tens of nm; i.e., the coils collapse almost entirely at the binding site, most likely because of multiple interactions. In contrast, the strong binding can be either associated with ABs becoming buried deep inside the PEG, i.e., full ternary adsorption in analogy with NPC proteins,[31] or possibly binding to a single chain closer to its free end.

On the basis of the SPR results, we tested to gate nanopores in 30 nm gold films sealed with PEG brushes[16] by introducing
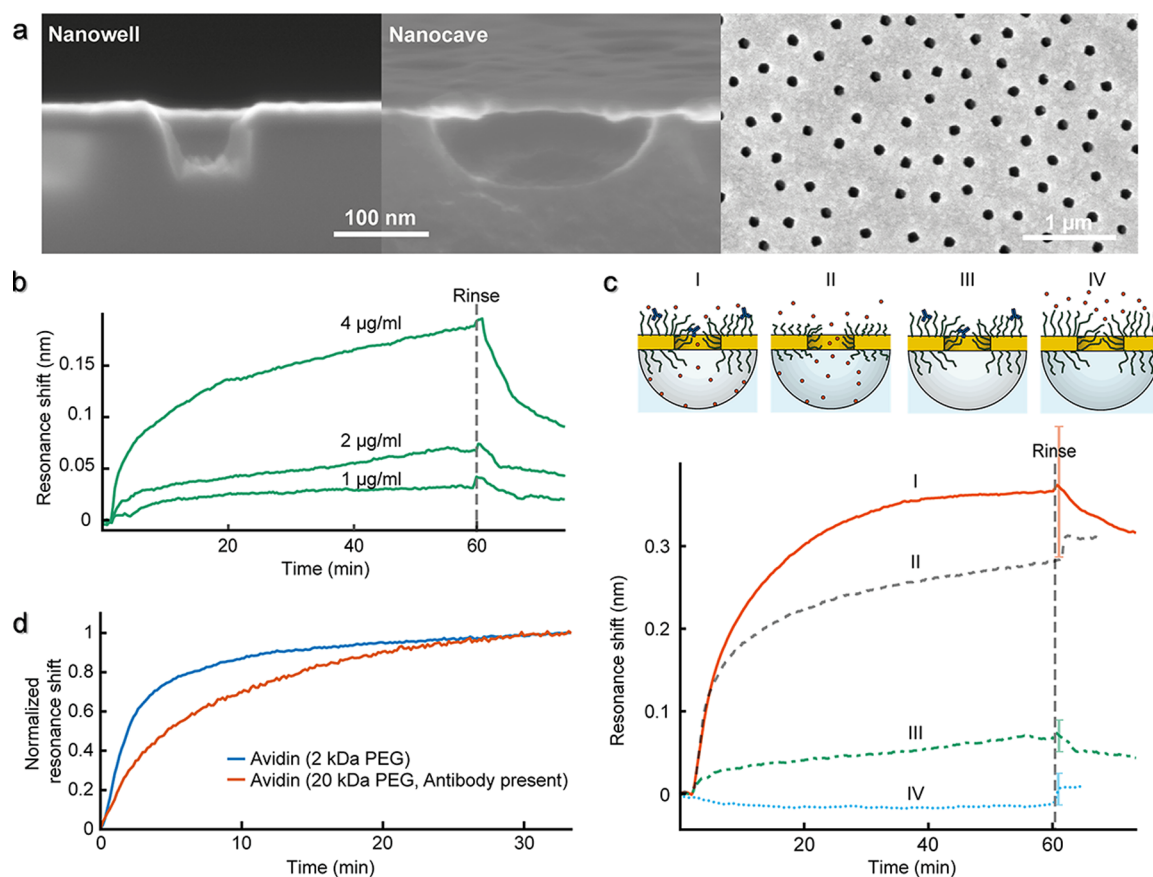
Figure 2. Gating nanopores by molecular recognition. (a) Images of the plasmonic nanopores used. (b) Plasmonic signal (resonance shift) from nanocaves functionalized with 20 kg/mol PEG upon AB injections at different concentrations. (c) Plasmonic signal when the AB (2 μg/mL) is introduced together with avidin (50 μg/mL), which adsorbs to silica underneath the apertures (I). For comparison we show the response from avidin for open pores, i.e., gold modified with 2 kDa PEG (II), the AB response (III), and the lack of a response for avidin without the AB (IV). Each situation is illustrated by a schematic. (d) Normalized response from avidin enabling comparison of translocation kinetics for open pores (2 kDa PEG) and gated pores (AB present). Note that results showing PEG sealing have been described in earlier work[16] and are presented again here for clarity.

relatively low concentrations of the AB, thereby promoting weak binding and brush collapse. As in previous work we used nanopore structures based on cavities in the silica support (Figure 2a),[32] which thanks to their plasmonic activity offer a simple way to monitor molecular binding with high resolution by spectroscopy in transmission mode.[17] The plasmonic signal emerges from the short-range ordering of the apertures, and hence, the system is suitable for probing multiple pores (in contrast to ionic current measurements). An average pore diameter in the range from 70 to 90 nm was used to ensure sealing by the 20 kDa PEG.[16] The AB binding to nanopores modified with PEG was first confirmed by introducing different concentrations followed by rinsing after 1 h of binding (Figure 2b). The association kinetics are slightly slower compared to SPR (Figure 1), which is because of diffusion (no steady flow for the nanoplasmonic sensor), while the dissociation rate is similar to the SPR data as expected. There was very little AB adsorption to silica under these conditions (Supporting Information), and hence, the signals originate from binding to the PEG brush.

The permeability with respect to protein translocation was tested by monitoring adsorption (or lack thereof) on the silica surface underneath the apertures using avidin (Figure 2c). As controls, we confirmed a clear signal from avidin adsorption to silica for "open" pores, i.e., gold modified with 2 kDa PEG[32]

(<7 nm thick), and no signal when using 20 kDa PEG.[16] Upon introducing avidin together with the AB the response was equal to the sum of the individual responses from the AB binding to PEG and avidin adsorbing to silica. Further, upon rinsing the signal went down by a value corresponding well to the reversible weak interaction. These results can only be explained by irreversible avidin adsorption inside the cavities, but this protein binding must be induced by the AB since avidin alone cannot penetrate the PEG barrier. Hence, the AB indeed operates as a key to gate the pores with respect to protein transport by molecular recognition. The minimum antibody concentration for which the pores became permeable to proteins was approximately 1 μg/mL. Upon rinsing the system and dissociating the ABs, the pores were again sealed to proteins, showing that the gating is reversible.

The plasmonic nanopore sensors can provide additional information through analysis of the binding kinetics (in addition to signal magnitude). Figure 2d compares the binding kinetics of avidin for open pores and gated pores, showing a small decrease in binding rate in good agreement with the time required for the ABs to establish equilibrium with PEG (Figure 2b). Thus, the real-time measurements show that the pores behave as "fully open" once the AB is bound; i.e., there is no difference in the transport rate compared to open pores that have 2 kDa PEG chains on the gold.
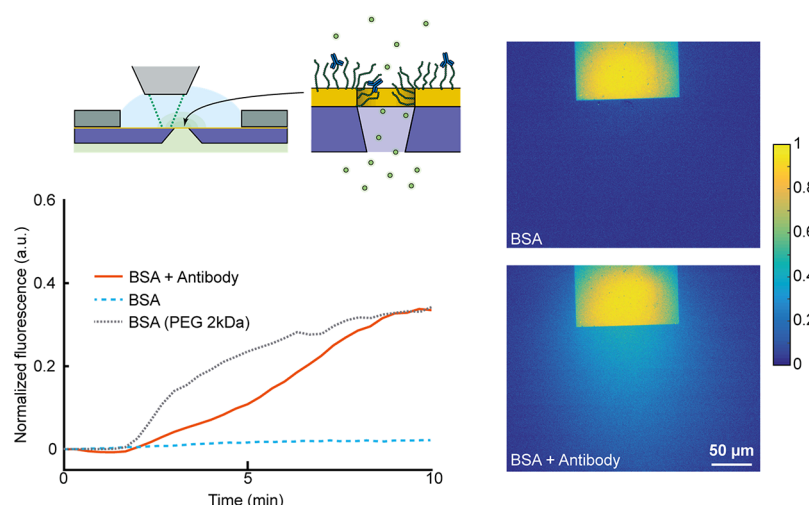
Figure 3. Complementary fluorescence microscopy showing gating of nanopore arrays in a membrane (120×120 μm^2). The time traces show the fluorescence intensity collected on the exit side after introducing BSA on the opposite side (flow starting at 0 min). The controls show the same data for membrane pores modified with short PEG (translocation occurs) and without the AB (no translocation). The pores are identical in shape to the nanowells in Figure 2a.
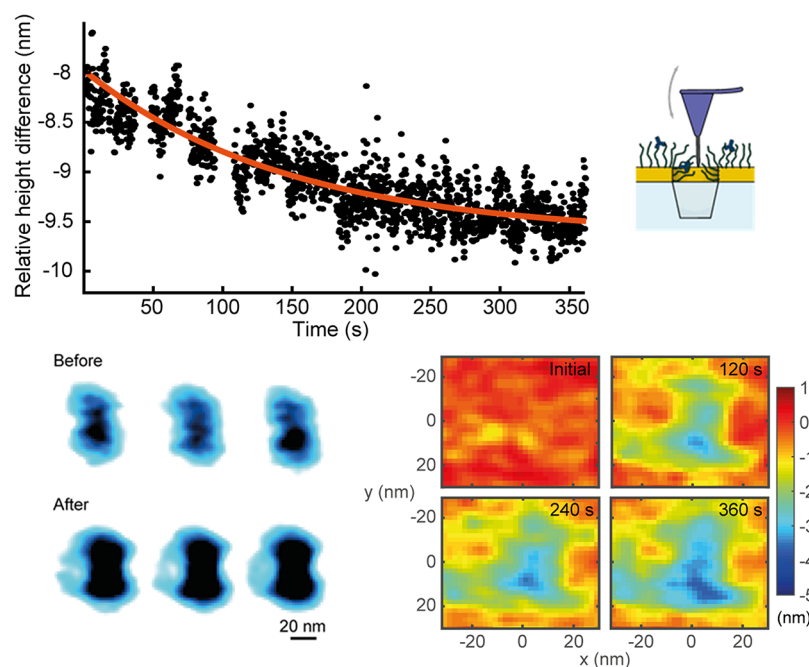

Figure 4. High-speed AFM on a single nanowell modified with 20 kDa PEG. The pore penetration depth (relative to the penetration on the planar surface) as a function of time after injection of AB (2 $\mu g/mL$). Data is averaged from a 700 nm^2 region in the pore center and compared to a region outside the pore of equal size. Representative frames before and after AB binding are also shown. The color maps show the difference in height compared to the initial frame.

To further verify gating by molecular recognition we used independent complementary techniques. Figure 3 shows the fluorescence intensity monitored next to a 50 nm silicon nitride membrane with plasmonic nanopores identical in shape to the nanowells (Figure 2a) upon introducing fluorescent bovine serum albumin (BSA) on the opposite side. There is no translocation of BSA through the pores when gold is modified with 20 kDa PEG, while the protein quickly diffuses through for the case of 2 kDa PEG as expected.[16] In the presence of the AB (4 $\mu g/mL$), BSA diffuses through the brush barrier with a short delay, again consistent with that measured by the nanoplasmonic sensor (Figure 2d). In addition to verifying the

gating principle, the results in Figure 3 show that the dynamic barrier control is compatible with large arrays, here, $>10^5$ pores in parallel (Supporting Information) connecting two liquid compartments. This shows that on-demand release of proteins on one side of the membrane is possible with a high molecular flux due to the ultrathin barrier.[3]

We also performed high-speed AFM while introducing the AB to nanowells functionalized with 20 kDa PEG to detect changes in brush morphology and repulsion. The change in penetration depth of the ultrasharp probe[9,16] (~5 nm radius of curvature) into the pore relative to the planar surface is plotted in Figure 4. After a few min the pore appears wider as shown

by the images, and the probe penetrates significantly deeper, consistent with an increased permeability of the brush barrier. Note that the time-dependent plot shows the average height difference of the pore region compared to the surrounding surface. A selection of individual frames show a higher penetration at certain locations (color maps in Figure 4), which could be due to a local brush collapse induced by a weakly bound AB. However, it should be kept in mind that the scan speed is not fast enough to capture all dynamics, and even the ultrasharp tip has a considerable size.[16] Thus, neither the initial nor the final images show an open pore in the physical sense, but there is clearly a significant reduction in the ability to repel the tip and a tendency among coils to gather up more toward the pore walls. An online video showing the morphology changes in real-time is available in the Supporting Information.

As a final result, we will show that a *single* AB per nanopore is sufficient for gating. First, based on SPR data (Figure 1), the surface coverage of ABs after ~10 min of exposure to a concentration of 4 μg/mL can be calculated[25] to be 860 nm^2 per molecule. This translates into less than 9 molecules inside an 80 nm aperture (the average diameter) in a 30 nm film (7500 nm^2 wall area). Further, the signal at the critical limit for gating (1 μg/mL) is 6 times lower (Figure 2b), which means that the average number of ABs per pore is 1.46, i.e., typically 1. It is also possible to utilize the plasmonic signal of the nanopores at the threshold of 1 μg/mL (0.03 nm) and compare it with the response from grafting the 20 kDa PEG (7.7 nm).[16] The PEG coverage is 897 ng/cm^2 on a planar surface,[16] and the ratio of the signals (0.004) thus gives an AB coverage of 3.5 ng/cm^2, which corresponds to 1.06 molecules per pore wall area. (The refractivity of proteins is slightly higher than for PEG,[25] suggesting an even lower number of ABs.) This direct quantification is quite accurate since the plasmonic response is linear, and the ABs obviously bind roughly at the same location as the PEG. One could argue that the pore regions may have a higher affinity for the AB due to changes in brush morphology.[33] However, this is highly unlikely because the pore walls are well-known to be the most sensitive region, and hence, the plasmonic response would be considerably higher. Indeed, previous work on very similar plasmonic nanopores has shown that one 60 kDa protein inside the cylindrical aperture corresponds to a signal of ~0.01 nm,[34] and the ABs which are almost three times heavier indeed give a three times higher response.

The fact that a single AB is sufficient for gating is arguably quite fascinating and shows that the number of PEG coils that represent the macromolecular barrier is quite low. Along the pore walls in the 30 nm thick gold film, coils grafted close to the openings will likely have their morphology altered,[33] and the thickness of the "truly repelling" brush barrier is likely closer to ~10 nm, i.e., comparable to the dimensions of the AB as expected for single molecule gating.

CONCLUSIONS

We have shown that, by introducing an AB to PEG-modified nanopores, it is possible to disrupt the entropic barrier presented by the polymer brush, which fully blocks translocation of proteins (to the extent that our systems can measure). The experimental data shows that a single antibody interacting weakly with the polymer is sufficient to collapse the brush and open a local path for proteins so that they diffuse through the pore. Remarkably, in this gated state the pores are fully permeable to proteins, i.e., as if there was no barrier present at all. In addition, the gating is reversible since the ABs can dissociate again. We are not aware of any previous experiments showing nanopore gating with respect to proteins by molecular recognition, although analogies exist for small molecules in drug delivery.[35] Certain DNA origami constructs can be switched to an "open" state by sequence-specific hybridization[36,37] but have never been used to regulate protein transport.

Still, further work is needed to elucidate details on the AB–PEG interaction and if it is influenced by the nanoscale geometry in the pore compared to the planar surface. It should also be kept in mind that this study only shows results for one type of PEG AB (E11), and other versions[23] may behave differently. The altered permeability of the PEG barrier due to interactions with ABs may be relevant for understanding the mechanism leading to accelerated blood clearance of PEG-modified substances.[21] It is intriguing that even if PEG is efficient in reducing nonspecific protein binding and enhancing biocompatibility the polymer may in fact be recognized by several antibodies,[38] which seem to be naturally emerging because of the frequent use of PEG.[39] This will most likely influence the PEG "stealth" effect, which is critical for making drug delivery vehicles bypass the immune system and yet surrounded by controversy.[40]

In the longer perspective, our results form a foundation for developing biomolecular filters which are also dynamic and responsive. In addition to nanopores, it will also be possible to regulate protein transport in long nanoscale channels by introducing polymer brush barriers at specific locations. Understanding and regulating the barrier mechanism of polymer brushes by specific attractive interactions may eventually provide highly selective filters that respond on demand as well as artificial shuttle-cargo systems that mimic biological systems.[8]

■ ASSOCIATED CONTENT

ⓢ Supporting Information

The Supporting Information is available free of charge on the ACS Publications website at DOI: 10.1021/acscentsci.8b00268.

> Additional experimental details, quartz crystal microbalance results, additional surface plasmon resonance data, images of membrane pores, details on kinetic modeling (PDF)
> High-speed AFM video (AVI)

■ AUTHOR INFORMATION

Corresponding Author
*E-mail: adahlin@chalmers.se.

ORCID ⊙
Andreas B. Dahlin: 0000-0003-1545-5860

Author Contributions
The manuscript was written with input from the coauthors. Approval to this submission has been given by all authors.

Notes
The authors declare no competing financial interest.
It should be noted that fabrication of "nanocaves" involves dipping samples in HF solution, which is highly toxic. Appropriate protective clothing is necessary.

■ REFERENCES

(1) Miles, B. N.; Ivanov, A. P.; Wilson, K. A.; Dogan, F.; Japrung, D.; Edel, J. B. Single Molecule Sensing with Solid-State Nanopores: Novel Materials, Methods, and Applications. *Chem. Soc. Rev.* **2013**, *42*, 15−28.

(2) Venkatesan, B. M.; Bashir, R. Nanopore Sensors for Nucleic Acid Analysis. *Nat. Nanotechnol.* **2011**, *6*, 615−624.

(3) Striemer, C. C.; Gaborski, T. R.; McGrath, J. L.; Fauchet, P. M. Charge- and Size-Based Separation of Macromolecules Using Ultrathin Silicon Membranes. *Nature* **2007**, *445*, 749−753.

(4) Lee, S. B.; Mitchell, D. T.; Trofin, L.; Nevanen, T. K.; Soderlund, H.; Martin, C. R. Antibody-Based Bio-Nanotube Membranes for Enantiomeric Drug Separations. *Science* **2002**, *296*, 2198−2200.

(5) Jovanovic-Talisman, T.; Tetenbaum-Novatt, J.; McKenney, A. S.; Zilman, A.; Peters, R.; Rout, M. P.; Chait, B. T. Artificial Nanopores that Mimic the Transport Selectivity of the Nuclear Pore Complex. *Nature* **2009**, *457*, 1023−1027.

(6) Kohli, P.; Harrell, C. C.; Cao, Z. H.; Gasparac, R.; Tan, W. H.; Martin, C. R. DNA-Functionalized Nanotube Membranes with Single-Base Mismatch Selectivity. *Science* **2004**, *305*, 984−986.

(7) Kowalczyk, S. W.; Blosser, T. R.; Dekker, C. Biomimetic Nanopores: Learning from and About Nature. *Trends Biotechnol.* **2011**, *29*, 607−614.

(8) Jovanovic-Talisman, T.; Zilman, A. Protein Transport by the Nuclear Pore Complex: Simple Biophysics of a Complex Biomachine. *Biophys. J.* **2017**, *113*, 6−14.

(9) Sakiyama, Y.; Mazur, A.; Kapinos, L. E.; Lim, R. Y. H. Spatiotemporal Dynamics of the Nuclear Pore Complex Transport Barrier Resolved by High-Speed Atomic Force Microscopy. *Nat. Nanotechnol.* **2016**, *11*, 719−723.

(10) Ku, J. R.; Stroeve, P. Protein Diffusion in Charged Nanotubes: "on-off" Behavior of Molecular Transport. *Langmuir* **2004**, *20*, 2030−2032.

(11) Yameen, B.; Ali, M.; Neumann, R.; Ensinger, W.; Knoll, W.; Azzaroni, O. Synthetic Proton-Gated Ion Channels via Single Solid-State Nanochannels Modified with Responsive Polymer Brushes. *Nano Lett.* **2009**, *9*, 2788−2793.

(12) Yameen, B.; Ali, M.; Neumann, R.; Ensinger, W.; Knoll, W.; Azzaroni, O. Ionic Transport through Single Solid-State Nanopores Controlled with Thermally Nanoactuated Macromolecular Gates. *Small* **2009**, *5*, 1287−1291.

(13) Hou, X. Smart Gating Multi-Scale Pore/Channel-based Membranes. *Adv. Mater.* **2016**, *28*, 7049−7064.

(14) Yu, S. F.; Lee, S. B.; Kang, M.; Martin, C. R. Size-based Protein Separations in Poly(ethylene glycol)-Derivatized Gold Nanotubule Membranes. *Nano Lett.* **2001**, *1*, 495−498.

(15) Wanunu, M.; Meller, A. Chemically Modified Solid-State Nanopores. *Nano Lett.* **2007**, *7*, 1580−1585.

(16) Emilsson, G.; Xiong, K.; Sakiyama, Y.; Malekian, B.; Ahlberg Gagner, V.; Schoch, R. L.; Lim, R. Y. H.; Dahlin, A. B. Polymer Brushes Inside Solid State Nanopores Form an Impenetrable Entropic Barrier for Proteins. *Nanoscale* **2018**, *10*, 4663−4669.

(17) Dahlin, A. B. Sensing Applications Based on Plasmonic Nanopores: The Hole Story. *Analyst* **2015**, *140*, 4748−4759.

(18) Coalson, R. D.; Eskandari Nasrabad, A.; Jasnow, D.; Zilman, A. A Polymer-Brush-based Nanovalve Controlled by Nanoparticle Additives: Design Principles. *J. Phys. Chem. B* **2015**, *119*, 11858−11866.

(19) Eskandari Nasrabad, A.; Jasnow, D.; Zilman, A.; Coalson, R. D. Precise Control of Polymer Coated Nanopores by Nanoparticle Additives: Insights from Computational Modeling. *J. Chem. Phys.* **2016**, *145*, 064901.

(20) Cheng, T. L.; Cheng, C. M.; Chen, B. M.; Tsao, D. A.; Chuang, K. H.; Hsiao, S. W.; Lin, Y. H.; Roffler, S. R. Monoclonal Antibody-based Quantitation of Poly(ethylene glycol-derivatized Proteins, Liposomes, and Nanoparticles. *Bioconjugate Chem.* **2005**, *16*, 1225−1231.

(21) Cheng, T. L.; Wu, P. Y.; Wu, M. F.; Chern, J. W.; Roffler, S. R. Accelerated Clearance of Polyethylene Glycol-modified Proteins by Anti-Polyethylene Glycol IgM. *Bioconjugate Chem.* **1999**, *10*, 520−528.

(22) Schneck, E.; Berts, I.; Halperin, A.; Daillant, J.; Fragneto, G. Neutron Reflectometry from Poly (ethylene-glycol) Brushes Binding Anti-PEG Antibodies: Evidence of Ternary Adsorption. *Biomaterials* **2015**, *46*, 95−104.

(23) Su, Y. C.; Chen, B. M.; Chuang, K. H.; Cheng, T. L.; Roffler, S. R. Sensitive Quantification of PEGylated Compounds by Second-Generation Anti-Poly(ethylene glycol) Monoclonal Antibodies. *Bioconjugate Chem.* **2010**, *21*, 1264−1270.

(24) Hyotyla, J. T.; Deng, J.; Lim, R. Y. H. Synthetic Protein Targeting by the Intrinsic Biorecognition Functionality of Poly-(ethylene glycol) Using PEG Antibodies as Biohybrid Molecular Adaptors. *ACS Nano* **2011**, *5*, 5180−5187.

(25) Emilsson, G.; Schoch, R. L.; Feuz, L.; Hook, F.; Lim, R. Y. H.; Dahlin, A. B. Strongly Stretched Protein Resistant Poly(ethylene glycol) Brushes Prepared by Grafting-to. *ACS Appl. Mater. Interfaces* **2015**, *7*, 7505−7515.

(26) Emilsson, G.; Schoch, R. L.; Oertle, P.; Xiong, K.; Lim, R. Y. H.; Dahlin, A. B. Surface Plasmon Resonance Methodology for Monitoring Polymerization Kinetics and Morphology Changes of Brushes - Evaluated with Poly(N-isopropylacrylamide). *Appl. Surf. Sci.* **2017**, *396*, 384−392.

(27) Munoz, E. M.; Correa, J.; Riguera, R.; Fernandez-Megia, E. Real-Time Evaluation of Binding Mechanisms in Multivalent Interactions: A Surface Plasmon Resonance Kinetic Approach. *J. Am. Chem. Soc.* **2013**, *135*, 5966−5969.

(28) Halperin, A.; Kroger, M. Ternary Protein Adsorption onto Brushes: Strong Versus Weak. *Langmuir* **2009**, *25*, 11621−11634.

(29) Cooper, M. A.; Williams, D. H. Kinetic Analysis of Antibody-Antigen Interactions at a Supported Lipid Monolayer. *Anal. Biochem.* **1999**, *276*, 36−47.

(30) O'Shannessy, D. J.; Winzor, D. J. Interpretation of Deviations from Pseudo-First-Order Kinetic Behavior in the Characterization of Ligand Binding by Biosensor Technology. *Anal. Biochem.* **1996**, *236*, 275−283.

(31) Schoch, R. L.; Kapinos, L. E.; Lim, R. Y. H. Nuclear Transport Receptor Binding Avidity Triggers a Self-Healing Collapse Transition in FG-nucleoporin Molecular Brushes. *Proc. Natl. Acad. Sci. U. S. A.* **2012**, *109*, 16911−16916.

(32) Malekian, B.; Xiong, K.; Emilsson, G.; Andersson, J.; Fager, C.; Olsson, E.; Larsson-Langhammer, E. M.; Dahlin, A. B. Fabrication and Characterization of Plasmonic Nanopores with Cavities in the Solid Support. *Sensors* **2017**, *17*, 1444.

(33) Tagliazucchi, M.; Szleifer, I. Stimuli-responsive Polymers Grafted to Nanopores and Other Nano-Curved Surfaces: Structure, Chemical Equilibrium and Transport. *Soft Matter* **2012**, *8*, 7292−7305.

(34) Xiong, K.; Emilsson, G.; Dahlin, A. B. Biosensing Using Plasmonic Nanohole Arrays with Small, Homogenous and Tunable Aperture Diameters. *Analyst* **2016**, *141*, 3803−3810.

(35) Aznar, E.; Oroval, M.; Pascual, L.; Murguia, J. R.; Martinez-Manez, R.; Sancenon, F. Gated Materials for On-command Release of Guest Molecules. *Chem. Rev.* **2016**, *116*, 561−718.

(36) Andersen, E. S.; Dong, M.; Nielsen, M. M.; Jahn, K.; Subramani, R.; Mamdouh, W.; Golas, M. M.; Sander, B.; Stark, H.; Oliveira, C. L. P.; Pedersen, J. S.; Birkedal, V.; Besenbacher, F.; Gothelf, K. V.; Kjems, J. Self-assembly of a Nanoscale DNA Box with a Controllable Lid. *Nature* **2009**, *459*, 73−75.

(37) Burns, J. R.; Seifert, A.; Fertig, N.; Howorka, S. A Biomimetic DNA-based Channel for the Ligand-controlled Transport of Charged Molecular Cargo Across a Biological Membrane. *Nat. Nanotechnol.* **2016**, *11*, 152−156.

(38) Ishida, T.; Kiwada, H. Anti-polyethyleneglycol Antibody Response to PEGylated Substances. *Biol. Pharm. Bull.* **2013**, *36*, 889−891.

(39) Chen, B. M.; Su, Y. C.; Chang, C. J.; Burnouf, P. A.; Chuang, K. H.; Chen, C. H.; Cheng, T. L.; Chen, Y. T.; Wu, J. Y.; Roffler, S. R. Measurement of Pre-existing IgG and IgM Antibodies Against Polyethylene Glycol in Healthy Individuals. *Anal. Chem.* **2016**, *88*, 10661−10666.

(40) Schottler, S.; Becker, G.; Winzen, S.; Steinbach, T.; Mohr, K.; Landfester, K.; Mailander, V.; Wurm, F. R. Protein Adsorption is Required for Stealth Effect of Poly(ethylene glycol)- and Poly-(phosphoester)-coated Nanocarriers. *Nat. Nanotechnol.* **2016**, *11*, 372−377.